

Large Scale Traces of Solar System Cold Dust on CMB Anisotropies

M. Maris¹*, C. Burigana², A. Gruppuso^{2,4}, F. Finelli^{2,4} and J.M. Diego³

¹INAF - Osservatorio Astronomico di Trieste, Via G.B. Tiepolo 11, I34100, Trieste, Italy

²INAF - IASF Bologna, Via P. Gobetti 101, Bologna, I40129, Italy

³IFCA, Instituto de Física de Cantabria (UC-CSIC), Avda. Los Castros s/n. 39005 Santander, Spain

⁴INFN, Sezione di Bologna, Via Irnerio 46, I-40126 Bologna, Italy

Accepted 2011 April 08. Received 2011 April 08; in original form 2010 October 04

ABSTRACT

We explore the microwave anisotropies at large angular scales produced by the emission from cold and large dust grains, expected to exist in the outer parts of the Solar System, using a simple toy model for this diffuse emission. Its amplitude is constrained in the Far-IR by the COBE data and is compatible with simulations found in the literature. We analyze the templates derived after subtracting our model from the WMAP ILC 7 yr maps and investigate on the cosmological implications of such a possible foreground. The anomalies related to the low quadrupole of the angular power spectrum, the two-point correlation function, the parity and the excess of signal found in the ecliptic plane are significantly alleviated. An impact of this foreground for some cosmological parameters characterizing the spectrum of primordial density perturbations, relevant for on-going and future CMB anisotropy experiments, is found.

Key words: Interplanetary Medium – (Cosmology): Cosmic Microwave Background – Infrared: Solar System – Submillimeter

1 INTRODUCTION AND TOY MODEL

The thermal emission from Interplanetary Dust Particles (IDPs), called Zodiacal Light Emission (ZLE), is a well known source of foreground in the (Far)IR sky. Recently Maris et al. (2006) discussed the use of the ZLE COBE model (Kelsall et al. 1998; Fixsen & Dwek 2002) below 1 THz to derive predictions for surveys dedicated to Cosmic Microwave Background (CMB), such as WMAP¹ and PLANCK². A weak, albeit significant, contribution at frequencies $\lesssim 857$ GHz will be likely detectable by PLANCK. The simple scaling law of Fixsen & Dwek (2002) predicts a small but not negligible contribution at 70–150 GHz, of particular interest in CMB studies. Theoretical estimates (Babich, Blake & Steinhardt 2007a,b) suggest that the collective emission of Kuiper Belt Objects (KBOs) and other minor bodies could produce imprints in CMB surveys.

CMB anisotropy maps derived from WMAP data are well consistent with the standard Λ CDM cosmological model. However, there are some intriguing deviations at large angular scales, such as those related to the angular power spectrum (APS) at low multipoles ℓ 's (Bennett et al. 2003a; Hinshaw et al. 2003; Spergel et al. 2003; Larson et al. 2010; Kim & Naselsky 2010a,b; Gruppuso et al. 2010). Other anomalies regard the alignment of low multipoles (Tegmark, Oliveira-Costa & Hamilton 2003; Gordon et al. 2005; Copi et al. 2007; Huterer 2006; Copi et al. 2007; Huterer 2006; Gruppuso & Burigana 2009; Gruppuso & Górski 2010) and to the North–South asymmetry of the APS with respect to the ecliptic plane (Tegmark, Oliveira-Costa & Hamilton 2003; de Oliveira-Costa et al. 2004; Copi et al. 2007; Huterer 2006). Moreover, Vielva et al. (2004) detected a localized non-Gaussian behavior in the southern hemisphere using a wavelet analysis technique, see also (Cruz et al. 2005), and Diego et al. (2010) recently identified an intriguing excess of emission in WMAP 5 years ILC map along the ecliptic plane. Their results will be discussed later in more detail.

If not produced by systematic effects (Tegmark, Oliveira-Costa & Hamilton 2003; Huterer 2006; Burigana et al. 2006; Gruppuso et al. 2007) these features could be of cosmological origin (Gordon et al. 2005; Ghosh et al. 2007) or effects produced by some foreground within the near Universe (Vale 2005; Cooray & Seto 2005; Inoue & Silk 2006a,b; Rakić, Räsänen & Schwarz 2006), the Galaxy (Frisch 2005), or the Solar System (Schwarz et al. 2004; Copi et al. 2007).

* E-mail: maris@oats.inaf.it

¹ <http://lambda.gsfc.nasa.gov/>

² <http://www.rssd.esa.int/planck>

Model	H_{KBOE}	WMAP Bands		
		Q	V	W
CM:	17.5°	2.905	3.016	3.362
WM:	17.5°	1.211	1.223	1.256
CM:	35°	2.698	2.698	3.100
WM:	35°	1.194	1.204	1.234
CM:	70°	2.064	2.122	2.303
WM:	70°	1.135	1.142	1.162

Table 1. Ratio between the quadrupole derived from the subtraction of the KBOE template from the WMAP 7 yr ILC map and the original WMAP map for the three WMAP Q, V, W bands and the considered models, using *anafast*. Models are the Cold Model (CM), with $T = 30$ K, $\tau = 3 \times 10^{-7}$ and the Warm Model (WM) with $T = 60$ K, $\tau = 3 \times 10^{-8}$.

It can not be excluded that some diffuse Solar System emission could contribute at low ℓ 's at WMAP frequencies (Schwarz et al. 2004; Copi et al. 2007). Such foreground would exhibit planar symmetry with respect to the ecliptic (or some plane slightly tilted with respect to it). According to (Far)IR measures, the “classical” ZLE is the thermal emission of sub-mm IDPs, with orbital radii within 5 AU, characterized by a $\approx \nu^4$ scaling below 1 THz (Fixsen & Dwek 2002). If larger particles exist, their emission would add to the classical ZLE, producing a signal at mm wavelengths, ranging between about 1/10 and 10 times the classical ZLE, with a less steep spectrum, $\approx 1/\nu$, as suggested by several models (Backman, Dasgupta & Stencel 1995; Stern 1996; Yamamoto & Mukai 1998; Moro-Martín & Malhotra 2002, 2003). Such particles can be produced by the erosion of KBOs due to mutual collisions or by the erosion of incoming interstellar dust and they should be located beyond Jupiter. They would be then colder and possibly larger than the IDPs responsible for the classical ZLE. Impact detectors onboard interplanetary probes reveal that such particles indeed exist (Landgraf et al. 2002), but very little is known about their nature.

Motivated by these considerations, we reconsider the problem of diffuse Solar System emission at cosmological frequencies, by introducing a toy model of emission from the KBO dust particles, that we will call in this paper KBO Emission (KBOE), and evaluating its implications for CMB observations.

To explore the effect of the KBOE on CMB maps we considered a toy model in which the emission is confined within a region of width H_{KBOE} , symmetric with respect to the ecliptic plane, with constant brightness inside and zero outside. Owing to the planar and cylindrical symmetry of the model, all the coefficients $a_{\ell m}$ for the multipole expansion in ecliptic coordinates of the KBOE will be zero except for those with even ℓ and $m = 0$. Then KBOE (and likewise ZLE) will just affect the map components with even ℓ . By denoting with $I_{\lambda}^{\text{KBOE}}(\hat{P})$, the KBOE for unit solid angle, integrated along a given pointing direction \hat{P} , notable relations can be derived for the sky-averaged KBOE, \bar{I}_{KBOE} , its variance over the sky and its quadrupole $a_{2,0}^{\text{KBOE}}$. Since in the model $I_{\lambda}^{\text{KBOE}}(\hat{P})$ is constant for \hat{P} within an angle $\pm H_{\text{KBOE}}/2$ from the ecliptic, defining $S = \sin(H_{\text{KBOE}}/2)$, we have $\bar{I}_{\text{KBOE}} = A_{\text{KBOE}}S$, $\text{var}(I_{\lambda}^{\text{KBOE}}) = A_{\text{KBOE}}^2 S(1 - S)$, and

$$a_{2,0}^{\text{KBOE}} = -A_{\text{KBOE}} \sqrt{5\pi} S(1 - S^2); \quad (1)$$

here A_{KBOE} is the constant value of KBO dust emission within the region. The maximum variance is $\text{var}(X) \leq A_{\text{KBOE}}^2/4$ and occurs for $H_{\text{KBOE}} = 60$ deg, while the $|a_{2,0}|$ maximum is $|a_{2,0}| \leq \sqrt{20\pi/27} A_{\text{KBOE}} \approx 1.53 A_{\text{KBOE}}$ occurring for $H_{\text{KBOE}} \approx 70.53$ deg. Flux variations can be translated in term of brightness temperature variations with the usual conversion factor $[\partial B_{\nu}(T)/\partial T]_{T=2.725\text{K}}$.

Detailed information about the distribution of dust in the outer Solar System to fix H_{KBOE} and A_{KBOE} is missing. A constraint on H_{KBOE} comes out from the distribution of inclinations of KBO orbits with respect to the ecliptic. KBOs are divided in two populations: classical KBOs with orbital inclinations within 10° about the ecliptic, and scattered KBOs with orbital inclinations within 40° about the ecliptic. In analogy with the distribution of dust from the erosion of Main Belt asteroids, we assumed that KBOs are a tracer of KBO dust and then of KBOE. Thus, we selected three possible representative values of $H_{\text{KBOE}} = 17.5^\circ, 35^\circ$ and 70° . The region of the ILC map affected by the KBOE in these three cases is shown in Fig. 1a (Note that this figure has been not included in the published version for editorial reasons.).

To constrain A_{KBOE} is a more complicated task, since it depends on details about grains such as their temperature, their size and their radial distribution, as well as their shape and their mineralogical composition. We rely on existing models predicting the possible sky-averaged KBOE brightness, leaving the development of a self-consistent model as a topic for a subsequent work. We choose as an example the model of Stern (1996), based on the production of dust in the KBO band by collisional disintegration of the KBOs. This model has the advantage to describe the sky-averaged KBOE in terms of two free parameters: the averaged dust temperature, T , ranging from about 10 K to 60 K and the sky-averaged optical depth, $\tau < 10^{-6}$. The model has been already constrained by the authors using IR data. Constraints come also from the microwave COBE/FIRAS data for the sky-averaged ZLE, I_{λ}^{ZLE} , (Fixsen & Dwek 2002). Fig. 1b compares the spectral energy distribution (SED) of the sky-averaged flux from KBOE, $I_{\lambda}^{\text{KBOE}}$, from the Stern (1996) prescription with I_{λ}^{ZLE} . All those combinations of (T, τ) values for which I_{λ}^{TOT} is upper-bounded by the gray band in Fig. 1b are acceptable. This is equivalent to take the $(I_{\lambda}^{\text{KBOE}}/I_{\lambda}^{\text{ZLE}})$ ratio at 350 GHz to be less than ≈ 6.5 . Fig. 1b shows that models with dust temperature $T = 10$ K, 30 K and 60 K and $\tau \leq 3 \times 10^{-7}$ are allowed by COBE/FIRAS data, and they predict at 93.5 GHz $I_{\lambda}^{\text{KBOE}}$ in excess of up to ≈ 80 times I_{λ}^{ZLE} . At frequencies above 1 THz, KBOE is one to three order of magnitudes below the classical ZLE, and it does not display any seasonal effect, so that its contribution to the bulk ZLE emission seen in COBE/DIRBE is negligible. Note that in the case of the most extreme models allowed by the COBE/FIRAS data it is possible to

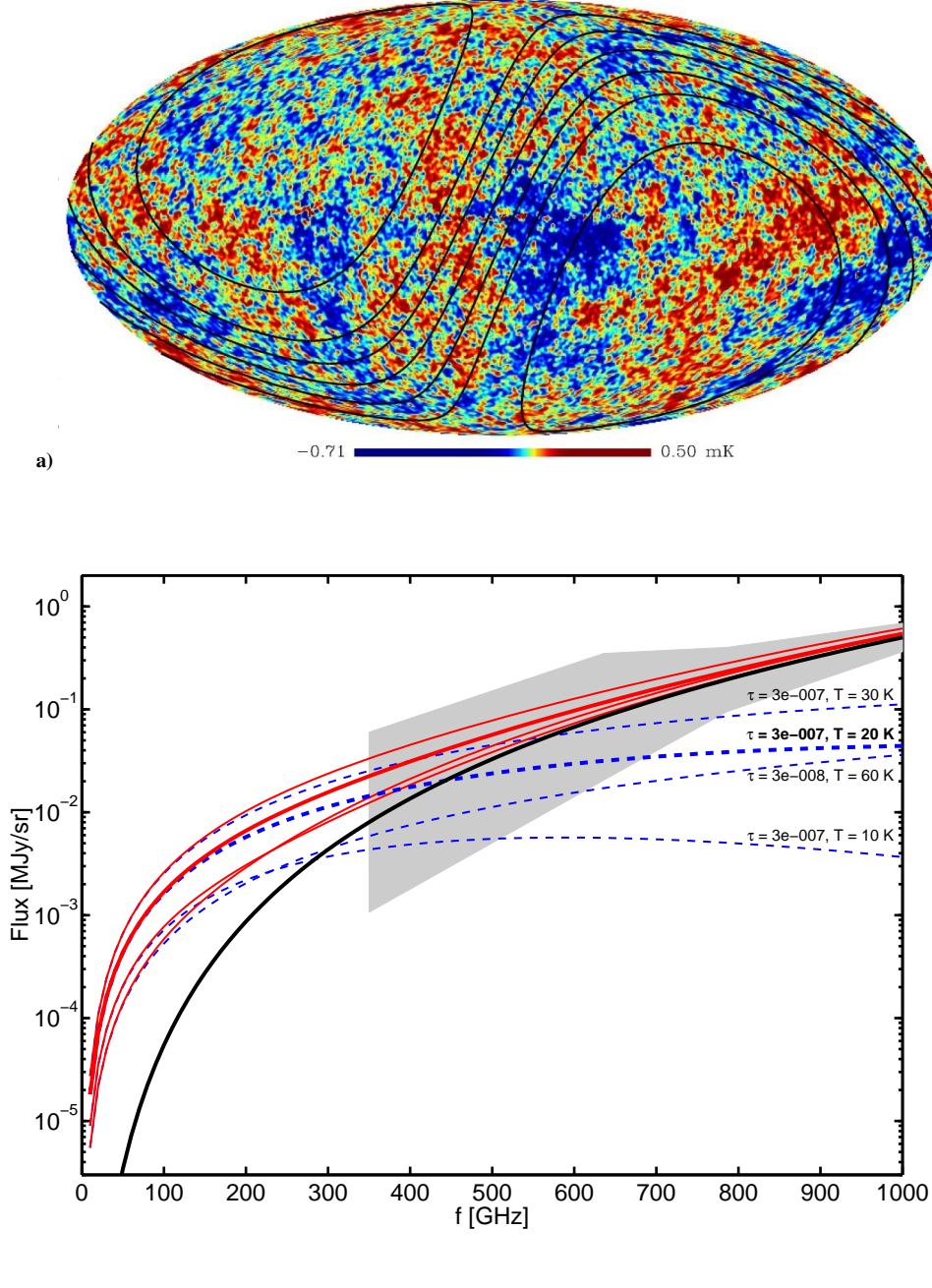


Figure 1. Panel a): the ILC map derived from WMAP 7 yr data. We displayed also with black lines the ecliptic plane and the three increasing regions where the KBOE is present in the case of our toy model, for three different increasing values of the height scale, $H_{\text{KBOE}} = 17.5^\circ, 35^\circ$ and 70° . Note that this figure has been not included in the published version for editorial reasons. Panel b): Comparison of ZLE fluxes compatible with COBE/FIRAS data (Fixsen & Dwek 2002) and a set of possible models of KBOE (Stern 1996). The black solid line shows the ZLE derived from the best fit model to COBE/FIRAS data and extrapolated to lower frequencies. The gray band represents a sketch of the allowed region obtained from the error bars in Fixsen & Dwek (2002). The blue dashed lines display four different models of KBOE corresponding to different values of τ and T . The resulting fluxes, sum of KBOE and ZLE, are represented by the red solid lines. Note that the classical ZLE (estimated on the basis of COBE data) is negligible in practice at WMAP frequencies, whereas KBOE might not be ignored.

predict a contribution to the quadrupole (see Eq. (1)) of up to $\approx 10^2 \mu\text{K}^2$, to be compared with the expected ZLE contribution less than $0.02 \mu\text{K}^2$ and the CMB quadrupole moment $\Delta T_{\text{CMB}, \ell=2} \approx 200 \mu\text{K}^2$ (WMAP Explanatory Supplement (2006), see also footnote 1).

How massive must be the debris disk to produce the KBOE? An estimate of the required Kuiper Belt mass to be converted in dust, $\mathcal{M}_{\text{dust}}$, can be readily derived from τ . From dynamical models of dust propagation and the distribution of objects in the Kuiper Belt it is possible to infer that Kuiper Belt Dust should be confined within $R_{\text{in}} \approx 30 \text{ AU}$ and $R_{\text{out}} \approx 50 \text{ AU}$. Since $T \propto 1/\sqrt{R}$ the grains could be considered approximately isothermal. As a further approximation it is possible to assume the numerical density of the dust n to be uniform between R_{in} and R_{out} . Assuming grains as spheres, with a typical diameter, a , unit emissivity efficiency, scattering cross-section given by their geometrical

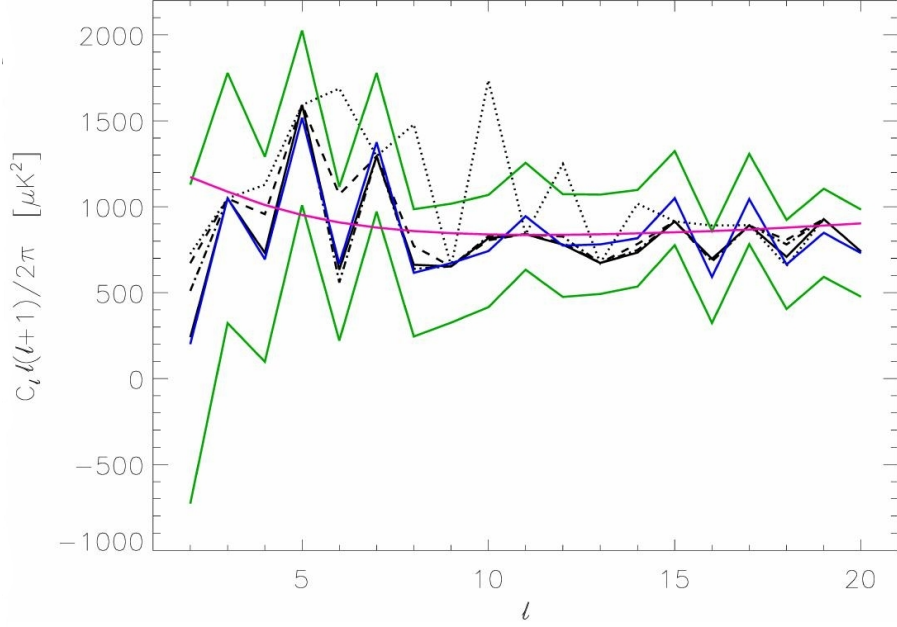


Figure 2. APS at low multipoles as derived by the WMAP team analyzing the ILC 7 yr map (blue solid line) with its 1σ errors (green solid lines); APS of the ILC 7 yr map derived using *Anafast* (black solid line); APS of the ILC 7 yr map after the subtraction of our KBOE template with $H_{\text{KBOE}} = 70^\circ$, 35° and 17.5° (black dotted–dashed line, dashed line, and dotted line, respectively). The dust model with $\tau = 3 \times 10^{-7}$ and $T = 30$ K (CM) and the V band is here considered. The red solid line shows APS of the best fit Λ CDM model for the WMAP 7 yr map.

cross section, then $n \approx 4\pi/[\pi a^2(R_{\text{out}} - R_{\text{in}})]$ and $\mathcal{M}_{\text{dust}} \approx (8\pi/9)\tau\rho a \sin(H_{\text{KBOE}}/2)[R_{\text{out}}^3 - R_{\text{in}}^3]/[R_{\text{out}} - R_{\text{in}}]$. Fragments should be composed largely of silicates, ices, and carbon compounds with densities ρ ranging between 1 and 3 gr/cm³. For $\tau \lesssim 3 \times 10^{-7}$, $H_{\text{KBOE}} \lesssim 70^\circ$, and $a \approx 1$ cm, $\mathcal{M}_{\text{dust}}$ varies between 6×10^{23} gr and 18×10^{23} gr, i.e. less than 0.14 Pluto masses.

2 ANALYSIS

The toy model outlined in Sect. 1 is exploited to assess its possible implications for CMB anisotropy statistical estimators and thus for cosmological models and parameters, under the assumption that such a kind of component present in the microwave maps, but it is hidden in the currently available CMB component maps.

Template production – According to the above assumption, we subtract our toy models from the available CMB anisotropy map. We will present here results obtained exploiting some KBOE toy model templates characterized by $H_{\text{KBOE}} = 17.5^\circ$, 35° , and 70° for two combinations of averaged dust temperature and sky-averaged optical depth: $\tau = 3 \times 10^{-7}$, $T = 30$ K (cold model, CM) and $\tau = 3 \times 10^{-8}$, $T = 60$ K (warm model, WM). These templates are computed in the ecliptic frame at the centers of the WMAP Q, V, and W frequency bands and generated at a resolution defined by the HEALPix (Górsky et al. 2005)³ parameter $N_{\text{side}} = 256$ (i.e. with a pixel size of about $13.7'$), appropriate to our large scale analysis. They are then convolved with a Gaussian symmetric beam with FWHM of 1° to match the beam resolution of the ILC 7 yr map released by the WMAP team and then transformed into Galactic frame. We have then subtracted the proper monopole to each template. At each frequency, we subtract our KBOE templates from the WMAP ILC 7 yr map (previously degraded at $N_{\text{side}} = 256$) to produce new CMB anisotropy maps cleaned by the adopted KBOE contribution.

Angular power spectrum – We extracted the whole-sky APS of the ILC 7 yr map released by the WMAP team and of the maps cleaned by the KBOE contribution described above using the publicly available HEALPix routine *anafast*, applying 3 iterations and subtracting monopole and dipole. The APS derived for ILC 7 yr map is compared with that released by the WMAP team. The results are shown in Table 1 and Fig. 2 for the low multipoles of interest here. As evident, no significant difference is found between the APS derived with *anafast* and with the finer approach applied by the WMAP team, thus probing that the results simply derived with *anafast* are accurate enough for the aims of this work. Table 1 shows that the subtraction of the KBOE template from the ILC map in the case of the CM implies a larger enhancement of the CMB quadrupole, while the effect, although present, is not so remarkable in the case of the WM. Also, this enhancement increases with the decrease of H_{KBOE} . These results do not depend significantly on the considered frequency channel because of the considered KBOE spectral shape. Thus, we will focus in particular on the V band, where Galactic foregrounds are minimum at large scales, and on the CM. In order to evaluate the probability that CMB quadrupole phases anti-correlate with the “deterministic” ones of

³ <http://healpix.jpl.nasa.gov/>

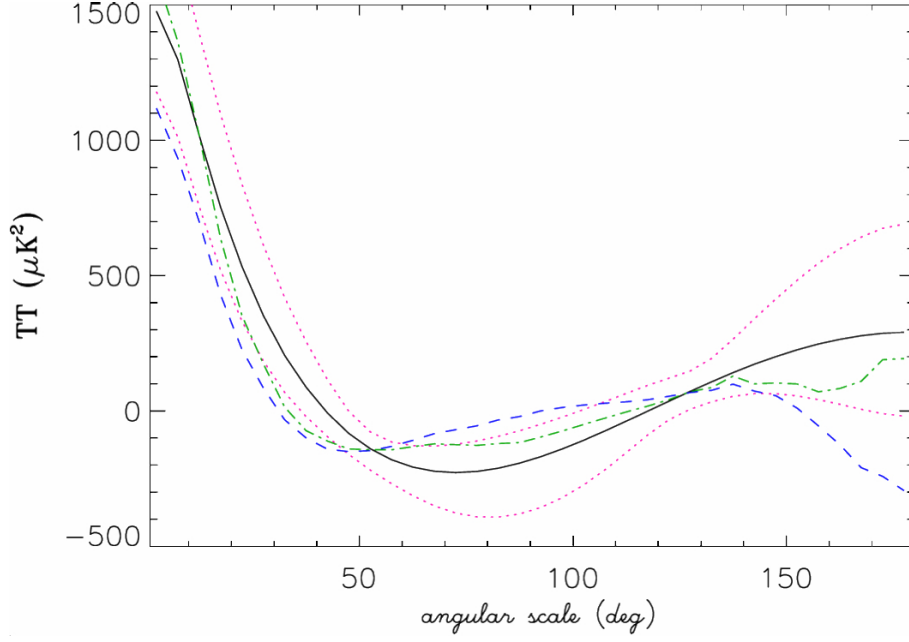


Figure 3. Two-points correlation function computed for maps at HEALPix resolution $N_{\text{side}} = 16$. The solid line displays the average of 10^5 MC realizations of CMB anisotropy maps extracted from the WMAP 7 yr best fit Λ CDM model APS shown in Fig. 2. The red dotted lines show the corresponding 1σ level fluctuations of the MC simulation. The blue dashed line refers to the ILC 7 yr map. The green dotted-dashed line refers to the map derived subtracting from the ILC 7 yr map one of our KBOE model, namely that obtained for the CM with $H_{\text{KBOE}} = 17.5^\circ$.

KBOE, we have performed a simple Monte-Carlo simulations. We extracted 10^4 random quadrupole realizations from the best fit of Λ CDM model obtained by WMAP 7 yr data and, for each of them, we have added our template and evaluated the modified quadrupole. We found that for about one out of three of realizations the band power, $\ell(\ell+1)C_\ell/(2\pi)$, of the quadrupole decreases from its primordial value, and, for example, for $\approx 11.5 - 13.4\%$ of the events it is lowered more than $300 \mu K^2$ depending on the specific CM considered⁴. These numbers do not depend strongly on the considered value of H_{KBOE} . This shows, reversely, that the probability of observing an ILC map whose quadrupole turn to be increased, once the KBOE template is removed, is not negligible. Fig. 2 reports the APS up to $\ell = 20$. Note that only the power of even multipoles is significantly affected, as expected since the geometrical symmetry of the KBOE component. For $H_{\text{KBOE}} = 70^\circ$ only the quadrupole turns to be significantly amplified, while for $H_{\text{KBOE}} = 35^\circ$ the power enhancement is important also at $\ell = 4$ and 6 and not negligible at $\ell = 8$. Remarkably, for $H_{\text{KBOE}} = 17.5^\circ$ the power increase is important for the even multipoles up to $\ell \approx 16$ (see also the following discussion on Parity). Note that the overall effect, when KBOE template is subtracted from the ILC map, is an increase of the resulting CMB power at even multipoles. This is for geometrical reasons, but related to the relative phases, or orientations, of $a_{\ell m}$ of ILC and of KBOE patterns.

Correlation function – The two point correlation function is defined as $C(\theta) = \langle T(\hat{n}_1)T(\hat{n}_2) \rangle_{\hat{n}_1 \cdot \hat{n}_2 = \cos(\theta)}$, where the symbol $\langle \dots \rangle_{\hat{n}_1 \cdot \hat{n}_2 = \cos(\theta)}$ stands for the average over an ensemble of realizations in which the directions \hat{n}_1 and \hat{n}_2 form an angle given by θ . In Copi et al. (2007) it is shown that at angular scales greater than about 60° the WMAP data occur in 0.025% of realizations of the concordance model (see also Copi et al. (2007); Hajian (2007); Copi et al. (2010) and references therein). In Fig. 3 we show $C(\theta)$ (black line) obtained through 10^5 MonteCarlo (MC) random realizations extracted from the WMAP 7 yr best fit Λ CDM model whose APS is displayed in Fig. 2. These random realizations properly take into account the anisotropic white noise level of the V band channel of WMAP 7 yr data. The resolution we have considered for this analysis is given by the HEALPix parameter $N_{\text{side}} = 16$ and the angle θ has been binned with a size of 5° . The red dotted lines show the corresponding 1σ level fluctuation of the MC simulation. The blue dashed line refers to the ILC 7 yr map. The green dotted-dashed line refers to the map derived subtracting from the ILC 7 yr map one of our KBOE model, namely that obtained for the CM with $H_{\text{KBOE}} = 17.5^\circ$. It is interesting to note how well the green line is (almost) always well consistent within 1σ level with the Λ CDM model whereas the blue line (i.e. the WMAP 7 yr ILC map) is often out of the 1σ contour, especially at large angular scale. This improvement is typical of our KBOE templates for the CM, while the templates for the WM do not change much the WMAP 7 yr ILC map correlation function.

Cosmological parameters – We quantify here the impact of the removal of the KBOE emission on cosmological parameters. The increase of the amplitude at low multipoles has interesting consequences on some of the cosmological parameters. For this purpose, we use the WMAP 7 yr likelihood code publicly available with the option of a pixel likelihood code at low resolution and substitute the WMAP 7 yr ILC map with the KBOE cleaned one. The Markov Chain Monte Carlo package CosmoMC (Lewis & Bridle 2002) is connected with this modified likelihood code. As shown in Fig. 4 the removal of a Solar System contamination (namely the CM with $H_{\text{KBOE}} = 35^\circ$) modifies slightly

⁴ Considering the fiducial Λ CDM model as a reference, the decreasing of at least $300 \mu K^2$ occurs for $\approx 30 - 36\%$ of the events.

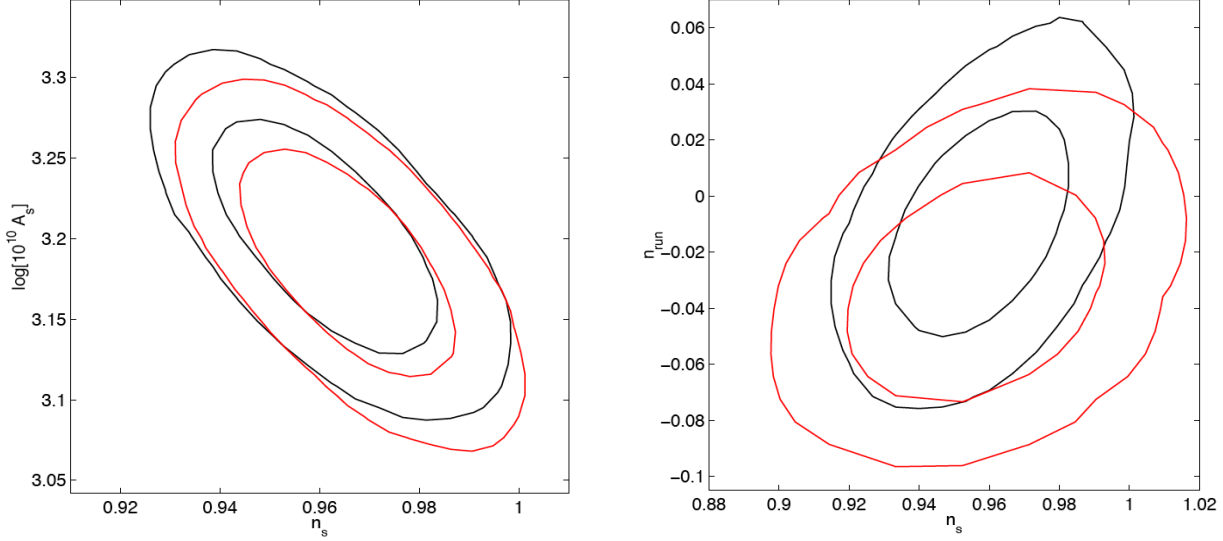


Figure 4. Two dimensional marginalised probability distributions for cosmological parameters by removing (black lines) or not removing (red lines) the KBOE template for the CM with $H_{\text{KBOE}} = 35^\circ$ (curves are the 68% and 95% confidence level). To the left (right) the plot for A_s (n_{run}) vs n_s for a standard Λ CDM model (including running of the scalar spectral index).

the amplitude and the spectral index of scalar perturbations (by choosing a pivot scale $k_* = 0.002 \text{Mpc}^{-1}$) in a standard Λ CDM scenario characterized by 6 cosmological parameters (plus the amplitude of the residual Sunyaev-Zeldovich effect): as expected by Fig. 2, a slightly larger value for the amplitude of primordial fluctuations is preferred by the larger amplitude of the temperature anisotropies at low ℓ 's. We find a little impact of the removal of this foreground on the constraints on the spatial flatness of our Universe. A larger effect is expected in extensions of the Λ CDM model in which the small value of the quadrupole plays a relevant role: Fig. 4 shows how smaller values of the running of the scalar spectral index $n_{\text{run}} = dn_s/(d \ln k)$ are preferred once the KBOE is removed (in this last case we have adopted an optimal pivot scale $k_* = 0.017 \text{Mpc}^{-1}$). It is important to note how the change in the mean value of n_{run} we obtain is 0.023 after removing the KBOE template. Such difference is comparable with the PLANCK sensitivity to n_{run} : it is therefore important to assess foreground contamination on large scales to infer on the primordial spectrum of density perturbations. Also, since correcting for KBOE the low multipole tail in TT is not so suppressed, including tensor perturbations in the analysis, we find that, the upper limit on tensor-to-scalar ratio of primordial perturbations, r_{TS} , is relaxed to $r_{\text{TS}} < 0.42$ (at 95%CL), compared 0.36 given in Larson et al. (2010). Note that this effect is due to the larger relevance of temperature information with respect to polarization in WMAP data.

Parity – One of the large scale anomalies is the Parity anomaly. For all-sky maps it is customary to expand the CMB temperature fluctuations $T(\hat{n})$ in terms of Spherical Harmonics $Y_{\ell m}(\hat{n})$ where \hat{n} is a direction in the sky, namely depending on a couple of angles (θ, ϕ) , $T(\hat{n}) = \sum_{\ell m} a_{\ell m} Y_{\ell m}(\hat{n}) \equiv \sum_{\ell} T_{\ell}(\hat{n})$, where in the last equation we have implicitly defined the maps $T_{\ell}(\hat{n})$ for each angular scale ℓ . Since under reflection (or Parity) symmetry $\hat{n} \rightarrow -\hat{n}$ the Spherical Harmonics behave as $Y_{\ell m}(\hat{n}) \rightarrow (-1)^{\ell} Y_{\ell m}(\hat{n})$, and the map $T_{\ell}(\hat{n})$ has even parity for even ℓ and odd parity for odd ℓ .

At large scales, we expect a Sachs-Wolfe plateau in terms of TT APS, therefore we roughly forecast the same amount of power in even and odd maps. It has been recently proved that for WMAP data at the large scales (Kim & Naselsky 2010a,b), precisely in the range of $\ell = 2 - 22$, the total power coming from even ℓ 's is unlikely smaller than the total power present in the odd ℓ 's. The probability related to this event is as low as 0.4% for the WMAP 7 yr data Kim & Naselsky (2010b) (see Gruppuso et al. (2010) for a temperature and polarization joint analysis). The analysis of this power asymmetry was first proposed in Land & Magueijo (2005b) to test the presence of foreground residuals since templates of dust, free-free or synchrotron emission possess a large Parity asymmetry. Also the KBOE template we propose in this paper, as well as the standard ZLE, is highly Parity-asymmetric. Therefore it is worth to study its possible impact on the WMAP ILC 7 yr map, of course under the assumption that a residual of the kind considered in the current paper, is present in the ILC map.

We consider the same estimator of Kim & Naselsky (2010a,b) defined as $r = P^+/P^-$, where $P^{\pm} = \sum_{\ell^{\pm}} \ell(\ell+1) C_{\ell}/2\pi$; here with $\sum_{\ell^{\pm}}$ we mean the sum over even or odd ℓ 's respectively in the considered range (here $2 - 22$ ⁵). We have extracted 10^5 random maps from the best fit model of WMAP 7 yr working at the HEALPix resolution $N_{\text{side}} = 64$ (i.e. all-sky maps of 49152 pixels). We have computed the r estimator for each random map and we have built the probability distribution function (pdf) for r , shown in Fig. 5. Note that the pdf for r does not peak around the value 1, but slightly larger since for the chosen ℓ -range, there are more terms at numerator than in the denominator. Vertical lines in Fig. 5. represent the values of r for the considered maps. Black vertical line (on left) stands for the WMAP 7 yr ILC map. The

⁵ We consider the same range of Kim & Naselsky (2010a) where it was shown the maximum of the anomaly. See also Bennett et al. (2010) for comments about “a posteriori” selections.

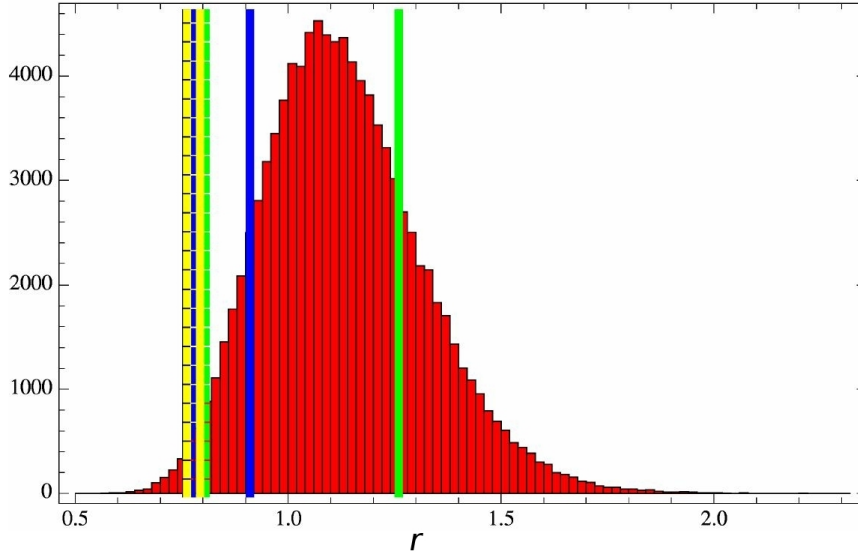


Figure 5. Parity anomaly of the estimator $r = P_+/P_-$ as defined in the text with $\ell_{max} = 22$. The histogram (in red) displays the distribution of r obtained from 10^5 MC realizations. Vertical lines correspond to the maps considered in this work: the black solid line (on the left) refers to the ILC 7 yr map; colored solid lines refer to the CM; colored dashed lines refer to the WM. Green, blue, and yellow lines are for $H_{KBOE} = 17.5^\circ, 35^\circ$, and 70° , respectively.

probability to have this value is as low as 0.91%⁶. When we remove our KBOE template from the maps we have the colored vertical lines. Green, blue, and yellow lines stand for $H_{KBOE} = 17.5^\circ, 35^\circ$, and 70° , respectively. Colored solid lines refer to the CM, colored dashed lines refer to the WM. Note that the probability associated to the green line (i.e. CM and $H_{KBOE} = 17.5^\circ$) is 77.1% and the probability associated to the blue line (i.e. CM and $H_{KBOE} = 35^\circ$) is 10.6%. The Parity anomaly is removed when these templates are properly taken into account. In the definition of the Parity estimator in the current paper we adopted $\ell_{max} = 22$, just for simplicity and since for that ℓ_{max} value the anomaly is remarkable. However, as shown in Kim & Naselsky (2010a,b); Gruppuso et al. (2010), in the WMAP TT spectrum there is a whole multipole range, rather than a single ℓ_{max} value, where the WMAP 7 parity anomaly holds. This dims significantly the case for posterior biasing. In analogy to what performed for the quadrupole, we have implemented a simple Monte-Carlo simulation in order to evaluate the probability that CMB even multipoles phases (up to $\ell_{max} = 22$) anti-correlate with the “deterministic” ones of KBOE. We extracted 10^4 random CMB realizations from the best fit of Λ CDM model obtained by WMAP 7 yr data and, for each of them, we have added our template and evaluated the modified spectrum. Hence, considering only the CM, we have found that the probability of lowering the estimator r is 24.7%, 7.05% and 0.07% for $H_{KBOE} = 70^\circ, 35^\circ$ and 17.5° , respectively. Similarly, we computed the probability of lowering the “even powers” up to $\ell_{max} = 22$ for some fixed threshold. For instance, for $H_{KBOE} = 70^\circ$ the probability to decrease the total even band powers of at least $300 \mu K^2$ with respect to the realization (or to the fiducial Λ CDM model) is 7.46% (43.46%), whereas it is 2.67% (23.26%) for $H_{KBOE} = 35^\circ$ and 0.01% (0.67%) for $H_{KBOE} = 17.5^\circ$. This shows that for H_{KBOE} larger than few tens of degrees the anti-correlation probability turns out to be not negligible. These numbers show that, contrarily to the quadrupole case discussed above, in this case the dependence on H_{KBOE} is important.

Alignments – We have seen how the removal of the KBOE template (for the CM) can reduce the unlikeliness of some estimators, as the C_ℓ and those related to them. Our preliminary tests carried out using a public code for the multipole vectors decomposition⁷ by Copi et al. (2004) show that this does not happen for the estimators based on $a_{\ell m}$ phases by means of which alignment anomalies are detected.

Ecliptic excess in WMAP data – In Diego et al. (2010), the authors look at the linear combination $V + W - 2Q$ of WMAP bands. In their analysis, the WMAP bands have been cleaned of Galactic contamination and the bright point sources have been masked. The linear combination $V + W - 2Q$ gets rid off the CMB signal completely and should contain a linear combination of the instrumental noise in each band, beam effects and residual Galactic and extragalactic foregrounds not accounted for in the cleaning (and masking) process. After masking out the Galactic plane, the authors found a significant large scale signal aligned with the ecliptic plane with a grey-body spectrum (see Fig. 1 in Diego et al. (2010)). A Galactic origin for this signal was ruled out due to the high latitudes where it was found. An extragalactic origin was also ruled out due the highly anisotropic distribution of this signal. In that paper it was suggested a possible origin in the ZLE but extrapolations from actual measurements from COBE/FIRAS predicted a much smaller signal than needed to account for the excess in the ecliptic plane. The present paper offers a fresh alternative to explain the excess by assuming a different population of larger dust grains. We have combined the signal expected from our KBOE models with the instrumental noise and beam of WMAP and built templates of the $V + W - 2Q$ maps. In Fig. 6 we show the predicted signal from the three CM models. The comparison with the signal detected by Diego et al.

⁶ This value is slightly larger than what quoted in Kim & Naselsky (2010a) that is 0.86%. This might be due to the details of the MC, like number of simulations, resolutions of maps and the considered FWHM.

⁷ See also <http://www.phys.cwru.edu/projects/mpvectors/>.

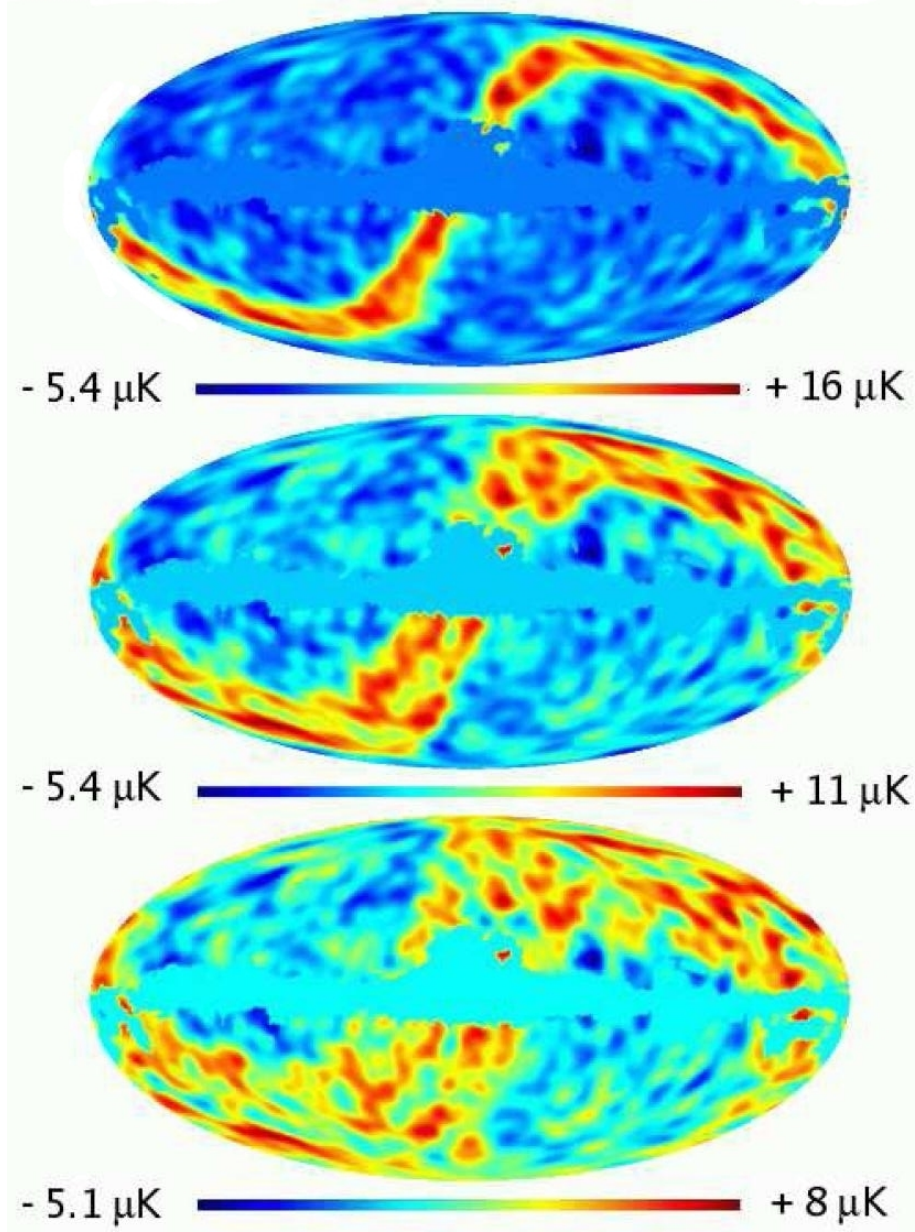


Figure 6. Predicted signal in the combination $V + W - 2Q$ from the CM with $H_{KBOE} = 70^\circ$ (bottom), $H_{KBOE} = 35^\circ$ (middle), and $H_{KBOE} = 17^\circ$ (top). The map units are μK and it has been smoothed with a 7° Gaussian. Compare this plot with Fig. 1 of Diego et al. (2010) based on WMAP data: the model with $H_{KBOE} = 70^\circ$ seems to agree better with the observations.

(2010) (see their Fig. 1) shows that the model with $H_{KBOE} = 70^\circ$ seems to agree better with the observations than the others. The areas near the Galactic plane show no evidence of excess appearing in WMAP data, that could be due to residual synchrotron emission. Note that while KBOE should be positive in $V + W - 2Q$, the synchrotron signal shows up as a negative signal in the combination $V + W - 2Q$.

3 CONCLUSION

We exploited a simple toy model for diffuse emission from cold and large dust grains expected to exist in the outer part of the Solar System and requiring only a modest amount of mass, with signal amplitudes, constrained in the Far-IR by COBE data, compatible with simulations existing in literature. We have produced and analyzed templates derived subtracting our toy model from WMAP ILC 7 yr maps to investigate on cosmological implications of such a foreground. We find that the anomalies related to the low quadrupole of the angular power spectrum, the two point correlation function, and the Parity are significantly alleviated. No significant impact has been found on low multipole alignments; of course, this does not exclude that more detailed models constructed in this framework could have consequences for these estimators.

It is interesting to note that there might be a relationship between the lack of effect of our model on the alignment of the low multipoles and the low amplitude of the quadrupole measured by WMAP. If the CMB intrinsic quadrupole is anti-correlated (i.e. with a similar pattern but opposite sign) with the ecliptic plane, any signal originating in our Solar System (like those considered in this paper) would *compete* with the CMB quadrupole, reducing its measured amplitude. On the other hand, the subtraction of the Solar System signal to the measured quadrupole would not change the orientation of the resulting signal since the subtraction operation transforms the anti-correlated signal in a correlated one and both patterns add up. A visual example of this can be found for instance in Fig. 9 of Diego et al. (2010) where also a hypothetical signal that traces the ecliptic plane is assumed. The same authors also demonstrate how signals in the ecliptic plane affect (significantly) only the even multipoles. Consequently, the octupole ($\ell = 3$) would remain basically unchanged. The KBOE is able to explain the excess of signal found in Diego et al. (2010), in particular for cold dust particles and for a high H_{KBOE} .

Finally, we showed that this foreground has an impact for some cosmological parameters characterizing the spectrum of primordial density perturbations, relevant for on-going and future CMB anisotropy experiments.

Clearly, the model needs to be improved in the future and tested against the data from the PLANCK satellite. Our analysis shows that it will be relevant to include, or at least to test, such component in the analysis of microwave anisotropy data at large scales.

ACKNOWLEDGEMENTS

We acknowledge the use of the Legacy Archive for Microwave Background Data Analysis (LAMBDA) supported by the NASA Office of Space Science. Some of the results in this paper have been derived using the HEALPix (Górsky et al. 2005) package. We acknowledge the use of the public code for the multipole vectors decomposition by Copi et al. (2004). Some of the simulations presented in this work have been performed using the computational facility of IASF Bologna and SP6 at CINECA. We acknowledge partial support by the ASI/INAF Agreement I/072/09/0 for the PLANCK LFI Activity of Phase E2 and the ASI contract I/016/07/0 COFIS. M.M. acknowledges partial support by FFO Ricerca Libera 2009 and 2010. C.B. warmly thanks P. Naselsky and D.J. Schwarz for stimulating conversations. JMD acknowledges support from the project AYA2010-21766-C03-01.

REFERENCES

- Babich, D., Blake, C.H., Steinhardt, C.L., 2007, ApJ, 669, 1406
- Babich, D., Loeb, A., 2007, NA, 14, 166
- Backman, D.E., Dasgupta, A., Stencel, R.E., 1995, ApJ, 450, L35
- Bennett, C.L., et al., 2003a, ApJS, 148, 1
- Bennett, C.L., et al., 2003b, ApJS, 148, 97
- Bennett, C.L., et al., arXiv:1001.4758 [astro-ph.CO].
- Bohren, C.F., Huffman, D. R., 1998, *Absorption and Scattering of Light by Small Particles* John Wiley & Sons, ISBN: 0471293407, New York, USA
- Burigana, C., Gruppuso, A., Finelli, F., 2006, MNRAS, 371, 1570
- Cooray, A., Seto, N., 2005, JCAP, 0512, 004
- Copi, C.J., Huterer, D., Starkman, G.D., 2004, PhRvD, 70, 043515
- Copi, C., J., Huterer, D., Schwarz, D., J., Starkman, G., D., 2007, Phys. Rev. D 75, 023507
- Copi, C., J., Huterer, D., Schwarz, D., J., and Starkman, G., D., 2009, MNRAS, 399, 295
- Copi, C. J., Huterer, D., Schwarz, D. J., Starkman, G. D., arXiv:1004.5602 [astro-ph.CO]
- Cruz, M., Martinez-Gonzalez, E., Vielva, P., Cayon, L., 2005, MNRAS, 356, 29
- Dennis M.R., 2005, J. Phys.A38:1653-1658
- Dennis, M.R., Land, K., 2007, arXiv:0704.3657 [astro-ph]
- de Oliveira-Costa, A., Tegmark, M., Zaldarriaga, M., Hamilton, A., 2004, PRD, 69, 063516
- Diego, J.M, Cruz, M., Gonzalez-Nuevo, J., Maris, M., Ascasibar, Y., Burigana, C., 2010, MNRAS, 402, 1213
- Finkbeiner D.P., Davis M., Schlegel D.J., 1999, ApJ, 524, 867
- Fixsen, D.J., Dwek, E., 2002, ApJ., 578, 1009
- Frish, P.C., 2005, ApJ, 632, L143
- Ghosh, T., Hajian, A., Souradeep, T., 2007, Phys.Rev.D, 75, 083007
- Gordon, C., Hu, W., Huterer, D., Crawford, T., 2005, Phys.Rev.D, 72, 103002
- Górski, K.M., Hivon, E., Banday, A.J., Wandelt, B.D., Hansen, F.K., et al., 2005, ApJ, 622, 759
- Gruppuso, A., Burigana, C., Finelli, F., 2007, MNRAS, 376, 907
- Gruppuso, A., Burigana, C., 2009, JCAP, 0908, 004
- Gruppuso, A., Górski, K. M., 2010, JCAP 1003, 019
- Gruppuso, A., Finelli, F., Natoli, P., Paci, F., Cabella, P., De Rosa, A., Mandolesi, N., will appear on MNRAS, arXiv:1006.1979 [astro-ph.CO]

- Hajian, A., 2007, arXiv:astro-ph/0702723
- Hinshaw, C., Spergel, D.N., Hill, R.S., et al., 2003, ApJS, 148, 135
- Huterer, D., 2006, New Astro. Rev., 50, 868
- Inoue, K.T., Silk, J., 2006a, ApJ, 648, 23
- Wilkinson Microwave Anisotropy Probe (WMAP): Three Year Explanatory Supplement*, M. Limon ed., et al (Greenbelt, MD: NASA/GSFC), available in electronic form at <http://lambda.gsfc.nasa.gov>
- Inoue, K.T., Silk, J., 2007, ApJ, 664, 650
- Kelsall, T., Weiland, J.T., Franz, B.A., Reach, W.T., Arendt, R.G., et al., 1998, ApJ, 508, 44
- Kim, J., Naselsky, P., arXiv:1002.0148 [astro-ph.CO]
- Kim, J., Naselsky, P., arXiv:1001.4613 [astro-ph.CO]
- Land, K., Magueijo, J., 2005, MNRAS, 362, L16-L19
- Land, K., Magueijo, J., 2005, Phys. Rev. D 72, 101302
- Landgraf, M., Liou, J.-C., Zook, H.A., Grün, E., 2002, ApJ, 123, 2857
- Larson, D., et al., 2010, arXiv:1001.4635 [astro-ph.CO]
- Lewis, A., Bridle, S., 2002, Phys. Rev. D, 66, 103511
- Maris, M., Burigana, C., Fogliani, S., 2006, A&A, 452, 685
- Moro-Martin, A., Malhotra, R., 2002, AJ, 124, 2305
- Moro-Martin, A., Malhotra, R., 2003, AJ, 125, 2255
- Rakić, A., Räsänen, S., Schwarz, D.J., 2006, MNRAS, 369, L27
- Schlegel, D.J., Finkbeiner, D.P., Davis, M., 1998, ApJ, 500, 525
- Schwarz, D.J., Starkman, G.D., Huterer, D., Copi, C. J. 2004, PRL, 93, 221301
- Spergel, D.N., et al., 2003, ApJS, 148, 175
- Spergel, D.N., Bean, R., Doré, O., et al. 2006, ApJS, 170, 377
- Stern, S.A., 1996, A&A, 310, 999
- Sykes, A.V., 1990, Icarus, 84, 267
- Tegmark, M., de Oliveira-Costa, A., Hamilton, A. J.S., 2003, PRD, 68, 123623
- Vale, C., 2005, astro-ph/0509039
- van Leeuwen, F., Challinor, A.D., Mortlock, D.J., Ashdown, M.A.J., Hobson, M.P., et al., 2002, MNRAS, 331, 975
- Vielva, P., Martinez-Gonzalez, E., Barreiro, R. B., Sanz, J. L., Cayon, L., 2004, ApJ, 609, 22
- Weeks, J., 2004, astro-ph/0412231
- Yamamoto, S., Mukai, T., 1998, Earth, Planets, Space, 50, 531